

HIRFL SEPARATED SECTOR CYCLOTRON PROGRESS

HIRFL Group (Presented by Wei Baowen)
 Institute of Modern Physics, Academia Sinica
 57 Nanchang Road, Lanzhou, China

Summary

The heavy ion research facility in Lanzhou (HIRFL) is a tandem cyclotron complex. It consists of four 52° sector separated cyclotron (SSC) with energy constant $k=450$ as the main accelerator and a three 33° spiral sector focusing cyclotron (SFC) with energy constant $K=69$ as the injector. The first beam is scheduled this year for SFC and at the end of 1988 for SSC. The progress of HIRFL is presented in this report.

Introduction

The heavy ion research facility in Lanzhou (HIRFL) is a tandem cyclotron complex. It consists of a four 52° sector separated cyclotron (SSC) with energy constant $K=450$ as the main accelerator and a three 33° spiral sector focusing cyclotron (SFC) with energy constant $K=69$ as the injector which is converted from an existing 1.5m conventional cyclotron. The low energy beam extracted from SFC goes through about 65m beam line including a stripper and two bunchers before injected into SSC. The high energy beam from SSC is guided into eight experimental equipments at the post beam line terminals in the experimental hall, among them, 6 for heavy ion nuclear physics and 2 for applied physics. Figure 1 shows the general layout of HIRFL. The design goal of this combination is set as follows:

-acceleration of ions from carbon to xenon with maximum energies of about 100Mev/u for light ions (C-,N-,N-,Ne-) and 5Mev/u for Xe-;

-beam intensity ranging from 10^{12} pps for light ions to 10^{10} pps for heavier ions;

-energy resolution being about 10^{-3} ;

-beam emittance being about 4π mm mrad.

Figure 2 presents the maximum energy per nuclear VS. mass number of HIRFL together with the major heavy ion cyclotron facilities in operation or under construction in some other laboratories in the world. As well known, the charge state Z of the beam through a stripper depends on beam energy E and the beam energy extracted from a cyclotron strongly depends on charge state:

$$E = K(Z/A)^2 \text{ Mev/u, } A = \text{mass number}$$

So developing an external ECR ion source for SFC has been planned. Although the use of high charge heavy ion source will be able to expand beam variety and energy range

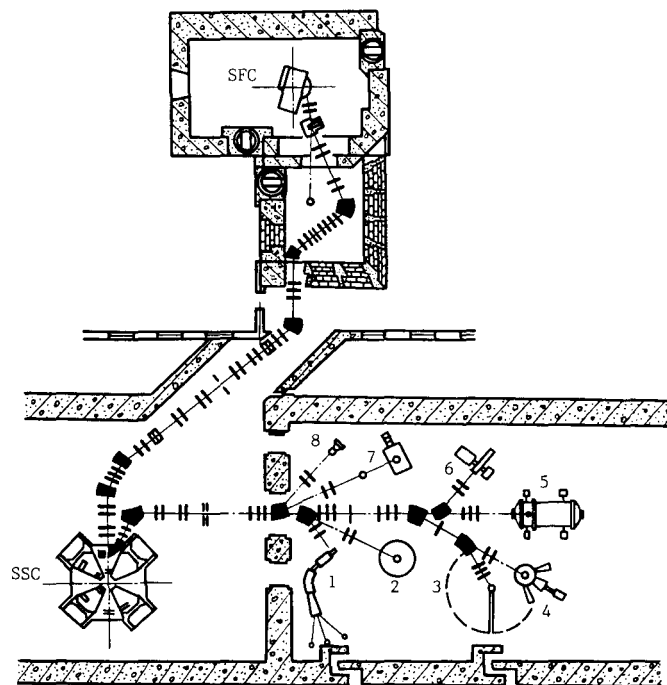


Figure 1: The general layout of HIRFL. 1- isotope separator, 2- on line γ -ray measuring devices, 3- heavy ion telescope with TOF, 4- position sensitive ionization chamber, 5- large scattering chamber for higher energy nuclear collision, 6 equipment for atomic physics study, 7 irradiation equipment with beam scanner, 8- fast chemical separation apparatus with He- jets.

of HIRFL, for example, tantalum to about 5Mev/u and xenon to about 19Mev/u, the PIG source will be maintained ready for putting in operation when ECR source is in maintenance or lower charge and higher intensity beam is needed.

IMP started researches on heavy ion nuclear physics by using 1.5m cyclotron modified to accelerate light heavy ions of C-,N- and O- to energies of about 73, 105 and 85Mev respectively in 1973. Then, a new project for constructing a more efficient heavy ion research facility in Lanzhou was proposed to Academia Sinica and it was approved at the end of 1976. The beam dynamic studies, model tests and technical design were completed around 1980 and the main parts of the mechanical and electrical components were ordered from factories around 1982. The accelerator building has been put in use since it was completed in November 1984. The sector magnets and supporting jacks, the coils and power sup-

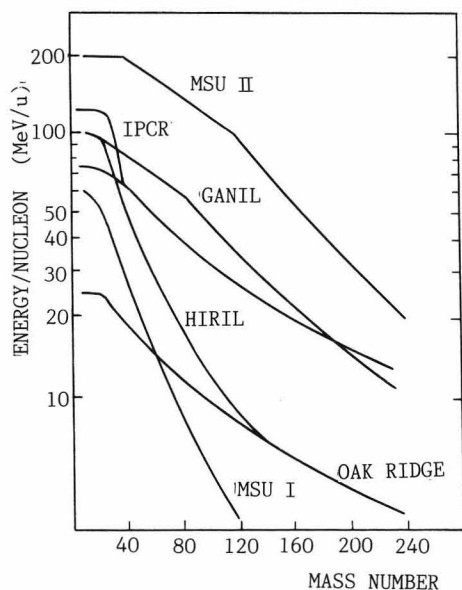


Figure 2: The maximum energy per nucleon VS. mass number together with the major heavy ion cyclotrons in operation or under construction in some laboratories in the world.

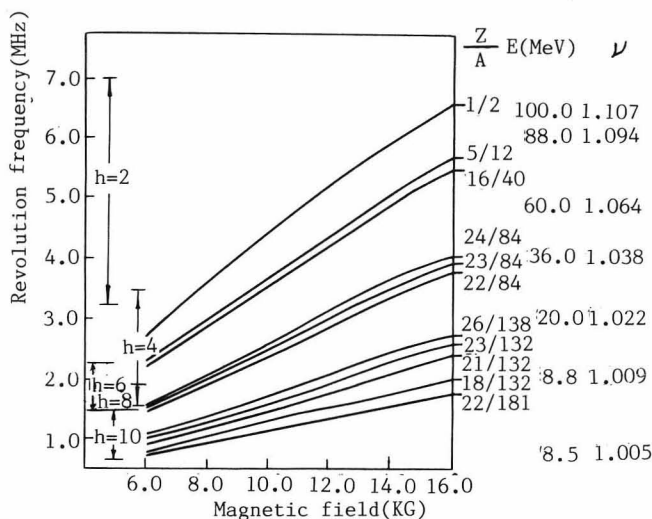


Figure 4: The relation between revolution frequency and magnetic field at the extraction mean radius of SSC. Z,A, γ ,E,h- same meaning with figure 3.

on accelerators for nuclear science and their applications and in 9th. international conference on cyclotrons and their applications 1-4. The progress of HIRFL is presented in this report.

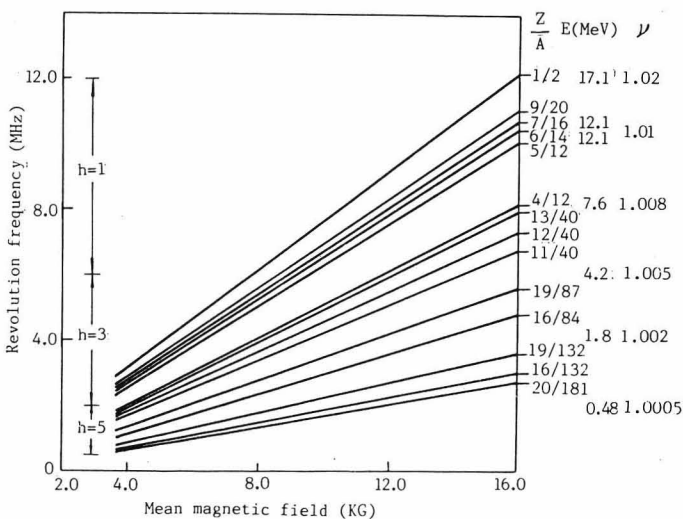


Figure 3: The relation between revolution frequency and mean magnetic field at the extraction radius of SFC. Z,A - charge and mass number, $\gamma=1+E/moc^2$, $moc^2=931MeV$, E - beam energy (MeV/u), $hfrev.=facc.$, h - harmonic number.

General description

Table 1 gives the main characteristics of HIRFL. The injection mean radius of SSC is 100 cm in order to have more room at the center region for installing the injection elements. However, the extraction radius of SFC being 75 cm is almost the best we could do as the diameter of pole base of original yoke is only 200cm, among them, 15cm lift for simulating the Rogowski profile and 10cm remained for margin region of the pole face. So that some times the two accelerators are operated in different frequencies and the synchronization and phase matching between them must be considered. Table 2 gives the matching parameters between SFC and SSC. There are four modes can be chosen covering the whole energy range from several MeV/u to 100 MeV/u with matching efficiency of 100%-50%. Table 3 gives the operating parameters and beam properties for some typical ions at the maximum energies. The associated acceleration of SFC and SSC will be started with equal frequency (mode A) for getting experience, so the beam planning of HIRFL is therefore decided in table 4.

-plies, the rf cavities and rf amplifiers, the vacuum chamber and pumping system, the injection and extraction system of SSC and new designed components of SFC have been delivered and installed on sites in the accelerator halls and basements. The remaining parts of beam lines and experimental equipments are now under fabricating and testing in chinese factories and our own workshop. The first beam is scheduled this year for SFC and at the end of 1988 for SSC.

The study and design of HIRFL were reported in China - Japan joint symposiums

The relations between revolution frequency and magnetic field at the extraction radius in SFC and SSC are shown in figure 3 and figure 4 respectively for different ions of Z/A on which the relativistic factor and then the extractd beam energy are concerned.

Injector SFC

The 1.5m cyclotron was closed down in February 1984 after operating about 20 years. The assembling of SFC was carried out properly. The concentricity of the upper

<u>Orbit parameters</u>		Operating pressure	10 ⁻⁷ torr
Injection mean radius	1.00m	Total gas load	10 ⁻² torr l/sec
Extraction mean radius	3.21m	Effective pumping speed	2 10 ⁵ l/sec
Radial betatron frequency	1.087-1.202	<u>Buncher</u>	
Vertical betatron frequency	0.742-0.864	Frequency range	26-56MHZ
Energy gain	10.3	Harmonic number	4
<u>Sector magnet</u>		Peak voltage	70KV
Number of sector	4	Number	2
Sector angle	52°	<u>Injector SFC</u>	
Magnet gap	10cm	Number of sector	3
Maximum field	16kG	Spiral angle	33°
Number of trim coil	36	Pole diameter	170.0cm
<u>Radio frequency</u>		Extraction radius	75cm
Frequency range	6.5-14MHZ	Maximum field	16kG
Number of Dee	2	Circular coil	12 pairs
Dee width	30°	Valley coil	4x3 pairs
Peak voltage	100-250kV	Dee Number	1
Rf power	240KW	Dee angle	180°
Harmonic number	2-10	Frequency range	6-18MHZ
Accelerating aperture	5cm	Peak voltage	100KV
Q-value	7000-12000	Rf power	200KW
<u>Vacuum</u>		Vacuum	5 10 ⁻⁶ torr
Volume of the vacuum chamber	100m ³		

Table 1: Main characteristics of HIRFL

Mode	R ₁ /R	n ₁ /n	h ₁ /h	f ₁ (mhz)	f (mhz)	F (Mc/s)	E (Mev/u)	η (%)
A	3/4	1/1	3/4	6.5-14.0	6.5-14.0	1.6-3.5	5.6-27.1	100
B	3/4	1/2	3/2	13.0-18.0	6.5-9.0	3.3-4.5	23.2-46.0	50
C	3/4	3/2	1/2	6.0-9.3	9.0-14.0	4.5-7.0	46.0-124.8	50
D	3/4	3/2	3/6	6.0-9.3	9.0-14.0	1.5-2.3	4.8-11.7	50

Table 2: Matching parameters between SFC and SSC. h₁, f₁ - harmonic number and radio frequency of SFC, h, f, F - harmonic number, radio frequency and revolution frequency of SSC, E - beam energy extracted from SSC, R₁ - extraction radius of SFC, R - injection mean radius of ssc, n₁f₁=nf, n₁, n - integral number, η = 1/n, matching efficiency.

Beam			12C	14N	40Ar	84Kr	132Xe
SFC	E	Mev/u	7.58	8.48	4.19	0.96	0.46
	ΔE/E		2 10 ⁻³	2 10 ⁻³	2 10 ⁻³	2 10 ⁻³	2x10 ⁻³
	ε	π mm.mrad.	12	12	12	12	12
	Bmax	kG	13.95	15.57	15.80	15.86	15.75
	h		1	1	3	3	3
	f	MHZ	8.04	8.50	18.00	8.46	6.00
	Z		4+	5+	10+	10+	11+
SSC	E	Mev/A	88	100	46	10	4.8
	ΔE/E		3 10 ⁻³	2 10 ⁻³	2 10 ⁻³	2 10 ⁻³	3 10 ⁻³
	ε	π mm.mrad.	4	4	4	4	4
	Bmax	kG	14.44	15.44	12.91	9.11	9.47
	h		2	2	2	4	6
	f	MHZ	12.06	12.76	9.00	8.64	9.00
	Z		6+	7+	16+	16+	23+
Mode			C	C	B	A	D

Table 3: The operating parameters and beam properties for some typical ions at the maximum energies of HIRFL.

	Accelerator	Mode	Ion source	Energy range (Mev/u)	Beam
1987	SFC		PIG	<10	C-Ar
1988	SFC		PIG	<10	C-Ar
1989	SFC+SSC	A	PIG	5.6-27.1	C-Kr
1990	SFC+SSC	A, B, C, D	PIG	4.8-100	C-Xe
1991	SFC+SSC	A, B, C, D	PIG, ECR	4.8-100	C-Ta

Table 4: Beam planning of HIRFL. The operating modes have been given in table 2.

and lower poles and the mechanical deviation of hill gaps of three pairs of the spiral sectors are limited less than 0.15mm. The magnetic field mapping was done by using 48 pieces of SBV 579 Hall probes mounted along a rotating arm included to the polar type azimuthal positioning apparatus. The first harmonic components in the regions of center, accelerating segment and pole fringe are 4 gauss, 3 gauss and 6 gauss respectively. The maximum deviation of the isochronous magnetic field is less than 5 gauss. So a good centerization of the beam orbits and a small center phase shift then a narrow energy spread could be expected^{5,6}.

The stability of DC power supplies of SFC is better than $5 \cdot 10^{-5}$ for main coil and about $1 \cdot 10^{-4}$ for circular and valley coils. The extraction system consists of three segments of electrostatic deflectors, among them, one has parallel electrode and two have hyperbolic electrodes, a focusing channel and two steering magnets. Three radial beam probes are inserted near the centerline of Dee stem, between and after the deflector respectively. 9 center phase probes are mounted along the radial direction with equal interval. Due to the limitation of the accelerator hall the stem of the single Dee has to make an angle of 50° to the accelerating gap. It introduces an asymmetrical distribution of about $\pm 4.5\%$ for the accelerating voltage with respect to the center of the machine. The effect on beam trajectories can be compensated by an equivalent amount of first harmonic in magnetic field given by the valley coils.

Sector magnet and isochronous field

Figure 5 shows the layout of trim coil and cross section of main and auxiliary coils for sector magnet of SSC. The ampere-turn of auxiliary coil is about 2.5% of that of main coil. The trim coil consists of 36 pairs of mineral insulated hollow conductors wound on the pole face following hard-edge approximation ion trajectories. Among them, 6 for compensating the effect of injection elements, 5 for compensating the local defects and 25 for isochronism.

Corresponding to radial coordinate r of the equilibrium closed orbit E.O. and isochronous magnetic field $B(r)$ along the sector hill, we define⁷:

$$r = k_r(r.B) \langle r \rangle$$

$$B(r) = k_b(r.B) \langle B \rangle$$

$$\langle r \rangle = \oint_{E_0} r ds / \oint_{E_0} ds$$

$$\langle B \rangle = \oint_{E_0} B ds / \oint_{E_0} ds$$

Using the isochronous condition $T = 2\pi m/q\langle B \rangle = \text{constant}$, we have

$$B(r) = k_b B_0 \gamma$$

$$B_0 = 2\pi f_{rev} Ag/Z \quad \text{gauss}$$

$$f_{rev} = k_r \beta c / 2\pi r$$

and

$$\beta \gamma = [(E/m_0 c^2)^2 + 2(E/m_0 c^2)]^{1/2}$$

$$\gamma = 1 + E/m_0 c^2$$

$$= (C/2 f_{rev}) / [(E/2\pi f_{rev})^2 - (r/l+b)^2]$$

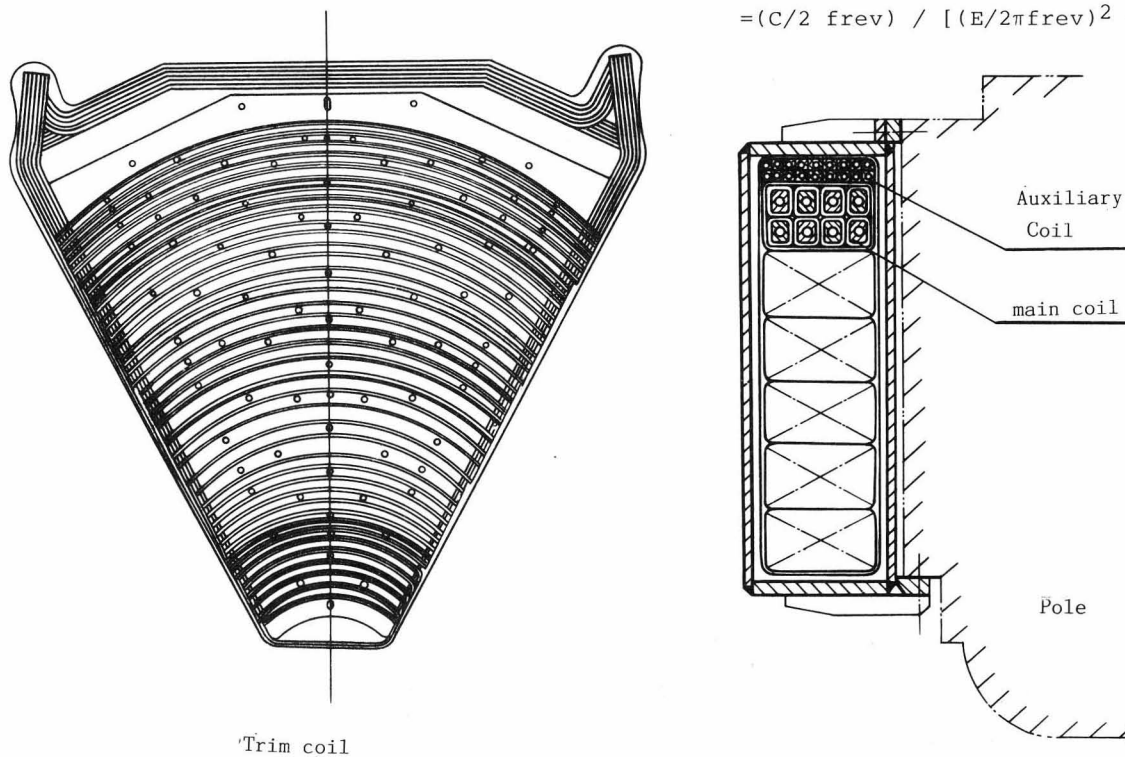


Figure 5: The layout of trim coil and cross section of main and auxiliary coils for sector magnet of SSC.

where, f_{rev} is revolution frequency, $g=1.036 \cdot 10^{-4}$, $m_0c^2=931\text{Mev}$, and $b=\sin(\delta-\alpha) / \sin \alpha = 0.74268$ for sector angle $2\alpha=52^\circ$.

From the measured ratios of k_r and k_b the required value of isochronous magnetic field $B(r)$ along the sector hill can be calculated for a given ion of (Z,A,E, f_{rev}) , then a set of main and trim currents are obtained by using the linear interpolation with the measured magnetic field maps and trim coil contributions. This method is perfect if k_r and k_b are the same for different isochronous fields, that means the geometries of closed orbits are the same for different ions and extracted energies. Furthermore, if the identity of 4 sectors is good enough, we can perform isochronism based on one sector calculation.

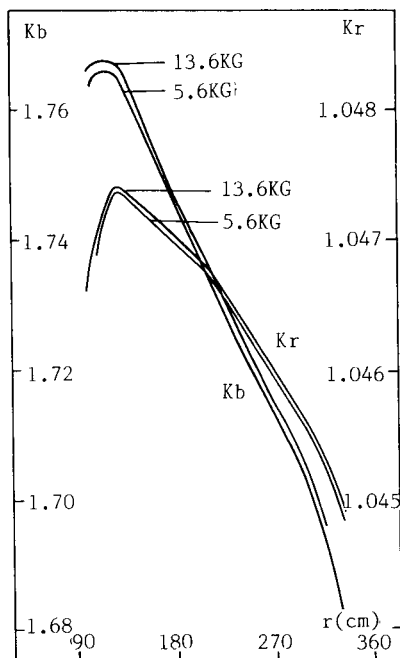


Figure 6: k_r and k_b vs. r for the magnetic field levels of 5.6 kG and 13.6kG respectively.

According to this consideration, the prototype test of sector magnet has been done by using 94 pieces of SBV 601 Hall probes mounted on a radial arm which is put on a moving ring with azimuthal positioning accuracy of about $0.5'$ and radial positioning accuracy of about 0.1mm for 360° mapping. The Hall probes are stabilized at $(35 \pm 0.1)^\circ\text{C}$ and calibrated by NMR method with a calibrating accuracy of about 10^{-4} . A 90° mapping needs about one hour as a micro computer is used for controlling and data acquisition. This apparatus will be also used for 4 sector measurement.

Figure 6 shows k_r and k_b vs. r for magnetic field levels of 5.6kG and 13.6kG respectively. They are almost the same for different levels and have varieties of about 0.003 for k_r and 0.1 for k_b from injection region to extraction region. In order to save the trimming currents, shims are added to both sides for each sector. The contribution of them to isochronous field is about 0.05. Figure 7 gives the mean field $\langle B \rangle$ vs. r with

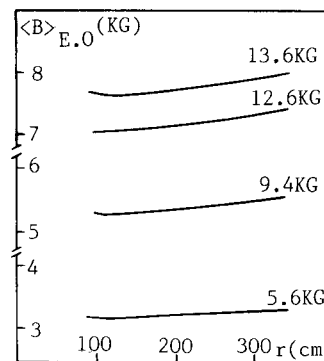


Figure 7: $\langle B \rangle$ vs. r with shim contribution.

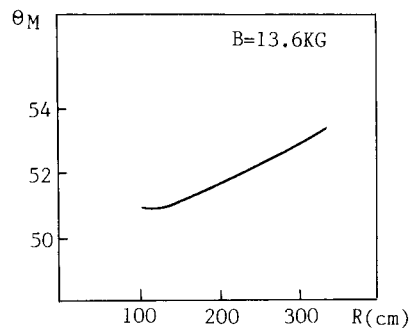


Figure 8: Magnetic angle vs. r with shim contribution.

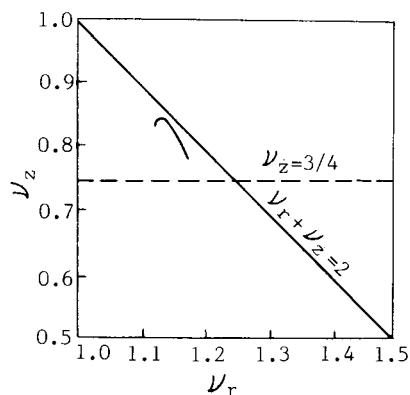


Figure 9: Betatron frequency for C^{6+} ion, 100MeV/u .

shim contraction. Figure 8 gives the magnetic angle with shim contribution. Figure 9 gives ν_z and ν_r curve for C^{6+} ion, 100MeV/u .

The stability of power supplies is about $5 \cdot 10^{-6}$ for main coil and about $5 \cdot 10^{-5}$ for auxiliary and trim coils.

Rf system

The rf cavity of ssc was tested under atmosphere by a small rf amplifier. Figure 10 shows the frequency range and figure 11 shows the voltage distribution vs. radius along the accelerating gap. The precision of the driving system of movable panel, the rotation of the trimmer loop and the

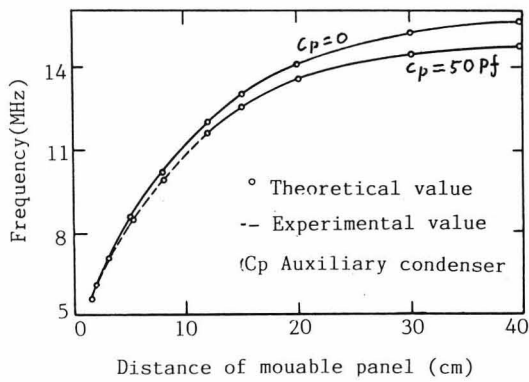


Figure 10: Frequency range of the rf cavity for SSC.

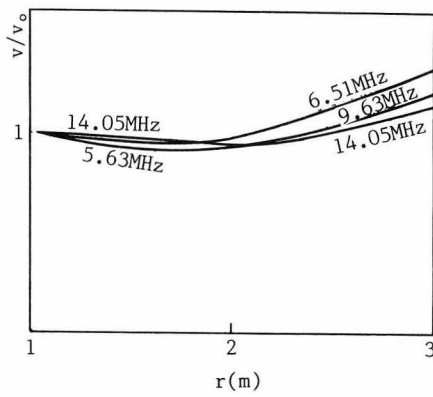


Figure 11: Voltage distribution vs. radius along the accelerating gap of the rf cavity for SSC.

combined operation of trimmer and panel were all checked satisfactorily. Two 120 kW rf amplifiers have successfully passed examination under full power 24 hour operation on a water cooling dummy load.

HIRFL has 5 rf cavities and amplifiers. The noise of rf amplifiers and the mechanical vibration of rf cavities introduce fast components of relative phase shift between cavities and the temperature variation of circumstance introduces slow components of that. So an elaborated phase stability system is thereby designed. In the design, the negative feedback loop with an electronic phase shifter is used to compensate the fast components, the mechanical and electronic phase shifters with a servocontrol system are used to compensate the slow one. One such rf chain including phase regulation loop, remote control coarse and fine phase shifters, frequency dividers, special designed digital phase meter, mastersynthesizer and a micro computer has been tested on site. The phase shift is less than 0.7° with a dynamic range of about $\pm 30^\circ$.

Vacuum system

The monolithic vacuum chamber (10m diameter and 4.5m height) has volume of about $100m^3$ and interior surface of about $1114m^2$ consisting of stainless steel $713m^2$,

mild steel $196m^2$, copper $200m^2$, antifricition material $4 m^2$ and elastomer $1 m^2$. The gas load after 10 hour pumping is about $2 \cdot 10^{-3} pa m^3/sec$ including metal outgassing 53%, non-metal outgassing 44% and leakage 3%. So an effective pumping speed of about $2 \cdot 10^2 m^3/sec$ is necessary to keep the chamber under required pressure of $10^{-5} pa$. The pumping system consists of 8 modified Balzers RKP 800 cryopumps as the main equipments and 2 pfeiffer TPH 5000 turbo molecular pumps as the auxiliary equipments used not only for pre-pumping the chamber to $10^{-4} pa$ but also for leak testing, cryopump regeneration and pumping helium. The liquid nitrogen consumption is about 30 l/hr.

Injection and extraction system

The injection beam goes through accelerating gap two times before injected into first orbit. It causes an increase of magnetic rigidity and about 7° of phase shift. First 10 turn of beam trajectories is iteratively calculated in normal way and reversely to match the injection condition respecting radial position r_0 , injection angle α_0 and magnetic rigidity G_0 . The parameter of r_0 and α_0 will be finally optimized after the machine is put in operation according to the orbit precession measured by radial beam probes. The perturbation field of bending magnets and stray field outside magnetic channels are compensated by shims and trim coils respectively.

	Xe	C
Z	22+	6+
E (Mev/u)	4.8	100
Turn Separation (mm)	10.5	2.6
Beam width (mm)	7.5	6

Table 5: Extraction turn separation and beam width for Xe and C without bump field.

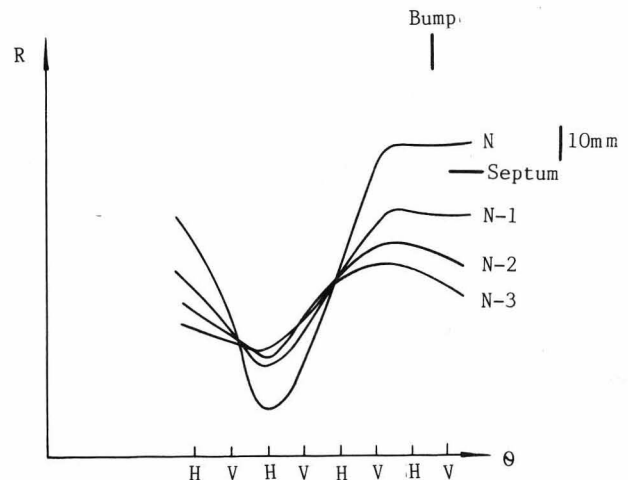


Figure 12: Extraction turn separation for C^{6+} , 100Mev/u under the effect of bump field. H - sector hill, V - centerline of the valley, N - turn order.

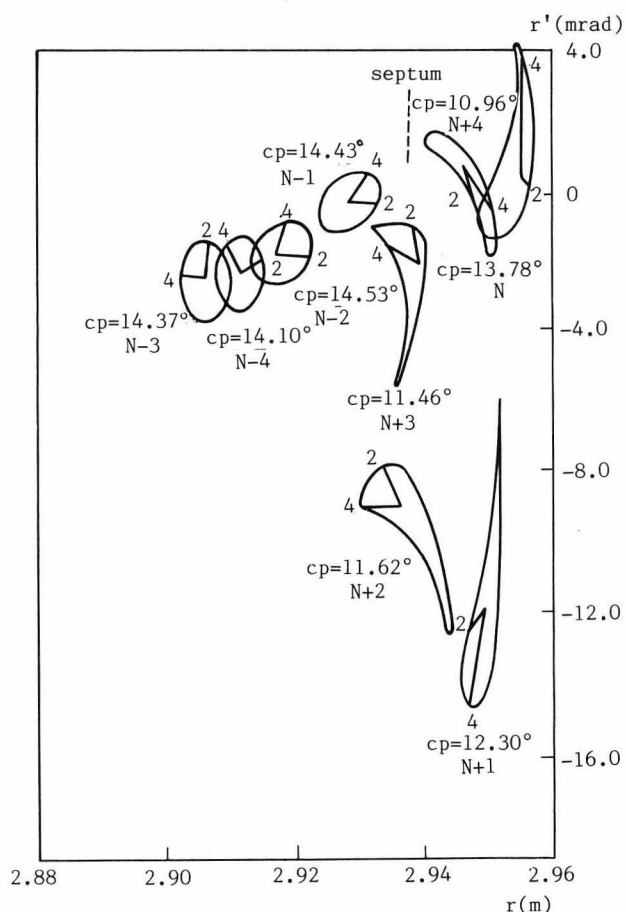


Figure 13: Radial phase plot for C^{6+} , 100MeV/u under the effect of bump field at the extraction region along the centerline of valley, in which a deflector is put. CP - center phase probe, N - turn order.

Single turn extraction will be no difficulty for heavier ions and lower energies as seeing in table 5. In the case of light ions and higher energies, the precessional extraction is adopted. A bump field has been set just before the entrance of extraction electrostatic deflector. Figure 12 and 13 give the turn separation and radial phase plot under the perturbation of the bump field.

Beam line from SFC to SSC

The design of the beam line has to match not only the transverse emittances but also the longitudinal phase ellipse. The beam line from SFC to SSC is operated in two modes: (1) one buncher with unit magnification is located at the middle of beam line to compensate the phase expand caused by energy spread; (2) two bunchers operate together, the second one is located at the one quarter place before SSC to compress the phase width at the expense of increasing energy spread. Figure 14 presents the longitudinal phase ellipsis.

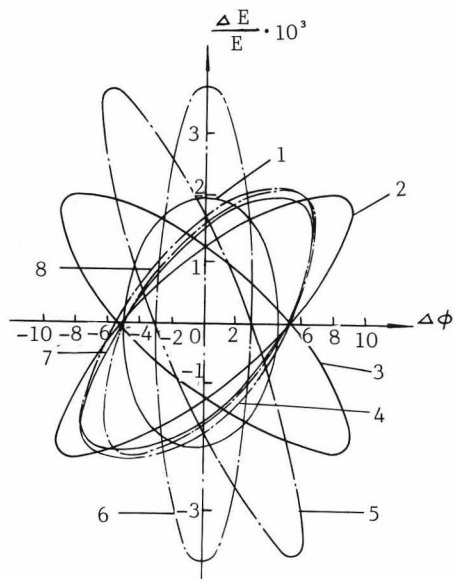


Figure 14: The longitudinal phase ellipsis of the beam in the transport line from SFC to SSC. Mode 2 - two bunchers, $h=4$, $\Delta\phi=+5^\circ$, $\Delta E/E=2 \cdot 10^{-3}$. 1 - SFC exit, 2 - buncher 1 entrance, 3 - buncher 1 exit, 4 - buncher 2 entrance, 5 - buncher 2 exit, 6 - SSC entrance, 7 - Str. entrance, 8 - Str. exit.

Beam diagnosis and control system

15 center phase probes are located along the centerline of west valley of SSC to optimize the isochronous field without intercepting the beam as 5 cm distance between upper and lower capacitive electrodes of the probe is large enough for beam going through. 4 movable radial beam probes are inserted through the return yokes of sector magnets used for centering the accelerating orbit. The probe head consists of main target, wire target, three finger target and NMR device. The main and wire targets measure the beam intensity, radial pattern and distribution. Three finger target measures the vertical distribution of the beam. The 4 NMR devices each inserted to the fixing point $r=2.5m$ along sector hills are used for marking and balancing the magnetic field levels of 4 sector magnets. The radial positioning accuracy of the beam probe is about 0.5mm.

The control system of HIRFL is based on CAMAC distributed intelligent control. The local control stations are designed according to HIRFL's subsystems such as injector, beam line, injection and extraction, magnet, vacuum, rf, diagnosis etc. The local stations are linked to the host computer Vax - 8300 by auxiliary controller in CAMAC crates of serial highway. The general layout of control system for HIRFL is shown in figure 15.

Experimental equipments and post beam line

The experimental hall is 26m width and 56m long. 8 experimental equipments for nuclear physics and applied physics have been designed at the post beam line terminals of HIRFL in the experimental hall. They are

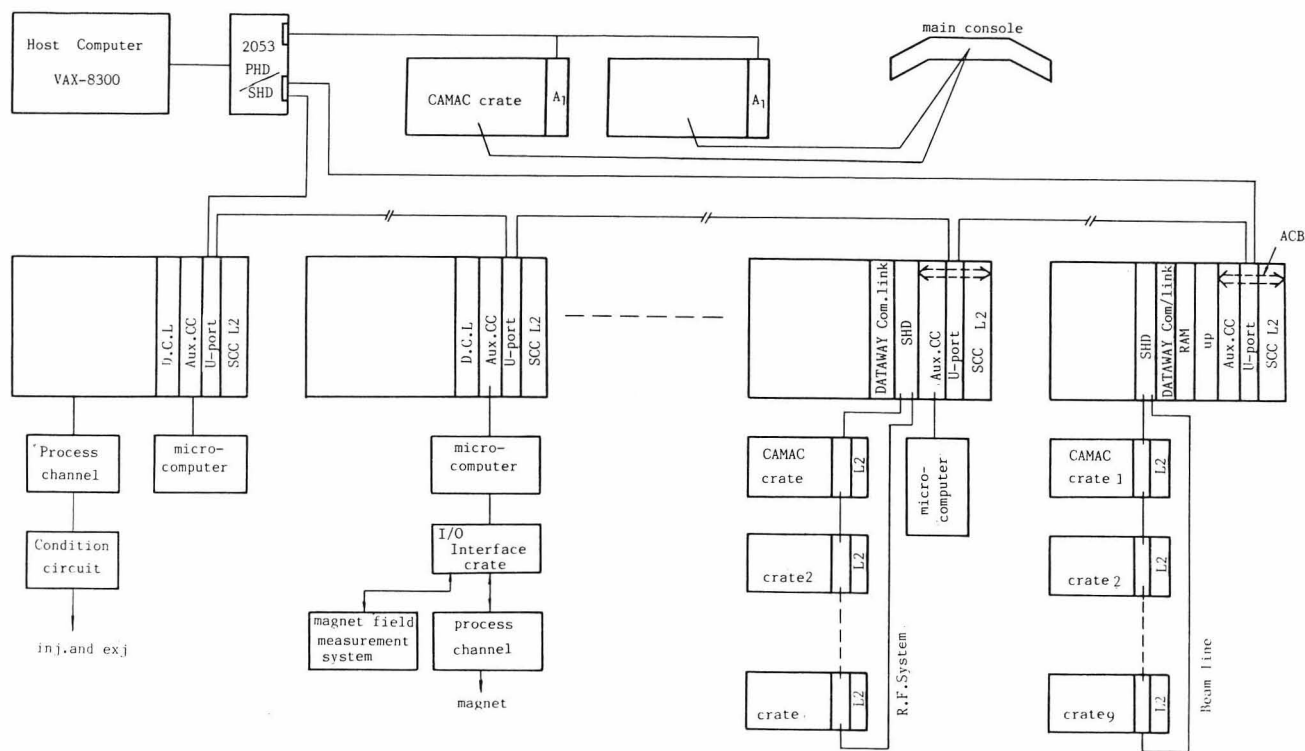


Figure 15: The general layout of control system for HIRFL.

as follows: (1) isotope separator, (2) on line γ -ray measuring devices, (3) heavy ion telescope with TOF, (4) position sensitive ionization chamber, (5) large scattering chamber for higher energy nuclear collision, (6) equipment for atomic physics study, (7) irradiation equipment with beam scanner and (8) fast chemical separation apparatus with He - jets.

The layout of post beam line is shown in figure 1. A 66° dipole and two doublets of quadrupoles are used to form a double waist at slit 1, then together with slit 2 form a collimator system, by which the beam emittance can be defined and unwanted beam can be cut off. Regarding to slit 1 as a starting point, the beam is delivered to each target with a beam emittance of about 4π mm.mrad. and a beam intensity as high as possible.

Reference

(1) Z.R.Ma etc., study and design for conversion of the 170cm sector focusing cyclotron from the existing 150cm classical cyclotron, Proc. 1st. Japan-China joint symposium on accelerators for nuclear science and their applications, Atami, 8-11 Sept. 1980, 63

(2) B.W.Weï, The present status of Lanzhou heavy ion research facility, Ibid, 1980, 390

(3) B.W.Weï, Present status of HIRFL, Proc. 9th. international conference on cyclotrons and their applications, caen, 7 - 10 sept, 1981, 23

(4) B.W.Weï, Progress in construction of HIRFL project, Proc. 2nd. China - Japan joint symposium, Lanzhou, 11 - 13 Oct. 1983, 25

(5) S.J.Zhang, Progress for 1.7m SFC, this conference

(6) Z.R.Ma, Design and measurement of SFC magnet, this conference

(7) M.Barre etc., Main results of the SSC's magnetic field mapping at GANIL, Proc. 9th. international conference on cyclotrons and their applications, 1981, 371

(8) S.X.Zhang, The vacuum system of SSC, this conference